Cosmic microwave background anisotropy from nonlinear structures in accelerating universes

Nobuyuki Sakai*

Department of Education, Yamagata University, Yamagata 990-8560, Japan

Kaiki Taro Inoue+

Department of Science and Engineering, Kinki University, Higashi-Osaka 577-8502, Japan

We study the cosmic microwave background (CMB) anisotropy due to spherically symmetric nonlinear structures in flat universes with dust and a cosmological constant. By modeling a time-evolving spherical compensated void/lump by Lemaitre-Tolman-Bondi spacetimes, we numerically solve the null geodesic equations with the Einstein equations. We find that a nonlinear void redshifts the CMB photons that pass through it regardless of the distance to it. In contrast, a nonlinear lump blueshifts (or redshifts) the CMB photons if it is located near (or sufficiently far from) us. The present analysis comprehensively covers previous works based on a thin-shell approximation and a linear/second-order perturbation method and the effects of shell thickness and full nonlinearity. Our results indicate that, if quasilinear and large ($\gtrsim$ 100 Mpc) voids/lumps would exist, they could be observed as cold or hot spots with temperature variance $\gtrsim 10^{-5}$ K in the CMB sky.

I. INTRODUCTION

Recently, much attention has been paid to generation of the cosmic microwave background (CMB) anisotropy due to nonlinear evolution of the gravitational potential, which is called the Rees-Sciama (RS) effect [1]. It has been argued that the RS effect only affects the angular power spectrum of the CMB anisotropy at relatively small angular scales $l \gtrsim 3000$ [2–4]. However, recent discoveries of the CMB anomalies such as octopole planarity, the alignment between quadrupole and octopole components [5], anomalously cold spots on angular scales ~10° [6], and asymmetry in the large-angle power between opposite hemispheres [7] hint that the RS effect due to large-scale structures could affect the CMB anisotropy at large angular scales as well [8]. This possibility is also indicated by a recent report that the density of extragalactic radio sources as projected on the sky is anomalously low in the direction towards the cold spot in the CMB map [9].

The signatures of the RS effect due to nonlinear voids/lumps in the Friedmann-Robertson-Walker (FRW) universe without a cosmological constant has been extensively studied in the literature [2–4]. Recently, the RS effect due to a quasilinear void/lump in the FRW universe with a cosmological constant has been studied using a thin-shell approximation [10] and a second-order perturbation method [11]. In order to check the validity and consistency, it is of great importance to extend the analyses to solve the Einstein equations without relying on these approximations.

In this paper, we study the RS effect due to nonlinear structures in flat universes with a cosmological constant by

solving the Einstein equations, which incorporate the fully nonlinear regime. Specifically we model a compensated spherical nonlinear void/lump by a family of Lemaitre-Tolman-Bondi (LTB) spacetimes and numerically solve the null geodesic equations with the Einstein equations. In Sec. II, we derive the Einstein equations and null geodesic equations for LTB spacetimes and model a compensating spherical void/lump with a smooth mass density profile. In Sec. III, we show some numerical results. Section IV is dedicated to concluding remarks.

II. MODEL AND BASIC EQUATIONS

A. Lemaitre-Tolman-Bondi spacetime

We consider a spherically symmetric spacetime with dust and a cosmological constant Λ, which satisfies Einstein equations,

$$G_{\mu\nu} + \Lambda g_{\mu\nu} = 8\pi G \rho u_\mu u_\nu, \qquad (2.1)$$

where $g_{\mu\nu}$, $G_{\mu\nu}$, G, ρ, and u_μ are the Riemannian metric tensor, the Einstein tensor, the gravitational constant, matter density, and the fluid 4-velocity, respectively.

In spherical coordinates (t, r, θ, ϕ), the general solutions are represented by the LTB metric,

$$ds^2 = -dt^2 + \frac{R'^2(t,r)}{1+f(r)}dr^2 + R^2(t,r)(d\theta^2 + \sin^2\theta d\varphi^2), \qquad (2.2)$$

which satisfies

$$\dot{R}^2 = \frac{2Gm(r)}{R} + \frac{\Lambda}{3}R^2 + f(r), \qquad (2.3)$$

*nsakai@e.yamagata-u.ac.jp
+kinoue@phys.kindai.ac.jp

$$\rho = \frac{m'(r)}{4\pi R^2 R'}, \qquad (2.4)$$

where $' \equiv \partial/\partial r$ and $\dot{} \equiv \partial/\partial t$. The solutions contain two arbitrary functions, $f(r)$ and $m(r)$. If we give $'\Lambda$, $\rho(t_i, r)$, and the local Hubble parameter $H(t_i, r) \equiv \dot{R}(t_i, r)/R(t_i, r)$ at the initial time $t = t_i$, $m(r)$ and $f(r)$ are determined by (2.3) and (2.4). The radial coordinate r has a gauge degree of freedom, $r \rightarrow r' = $ [any function of r]; here we define r as the areal radius at the initial time: $R(t_i, r) = r$.

Once $m(r)$ and $f(r)$ are determined, the evolution of R is given by (2.3) numerically. Differentiating (2.3) with respect to r, we obtain

$$\dot{R}' = \frac{1}{2\dot{R}}\left(\frac{2Gm'}{R} - \frac{2Gm}{R^2}R' + f' + \frac{2}{3}\Lambda RR'\right), \qquad (2.5)$$
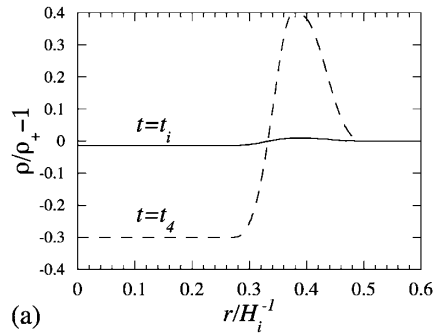
which is the evolution equation of R'. Although R' can be calculated also by the finite difference of R with respect to r, the integration of (2.5) with respect to t gives better precision for R'.

B. Modeling a void/lump

Our model is composed of three regions: the outer flat FRW spacetime (V_+), the inner negatively/positively curved FRW spacetime (V_-), and the intermediate shell region (V_s). In $V_\pm$, the field equations (2.3) and (2.4) reduce to the Friedmann equations,

$$H_+^2 = \frac{8\pi G\rho_+}{3} + \frac{\Lambda}{3}, \qquad \rho_+ \propto \frac{1}{a_+^3}, \qquad (2.6)$$

$$H_-^2 = \frac{8\pi G\rho_-}{3} + \frac{\Lambda}{3} + \frac{C^2}{a_-^2}, \qquad \rho_- \propto \frac{1}{a_-^3}, \qquad (2.7)$$

where $C \equiv \sqrt{f(r_-)}/r_-$ is a constant. Here $r = r_\pm$ denotes the boundary between $V_\pm$ and V_s whereas $a_\pm$, $H_\pm$, and $\rho_\pm$ simply mean the quantities in $V_\pm$.

The shell V_s is constructed by the LTB spacetime in such a way that $m(r)$ and $f(r)$ are continuous through $V_\pm$. At the initial time $t = t_i$, we assume that $\rho_- \approx \rho_+$, $H(t_i, r) = $ const, and the matter density profile is given by

$$\rho(r) = \begin{cases} \rho_- & \text{for } r \le r_-, \\ \frac{\rho_c - \rho_-}{16}(3X_-^5 - 10X_-^3 + 15X_- + 8) + \rho_- & \text{for } r_- \le r \le r_c, \\ \frac{\rho_+ - \rho_c}{16}(3X_+^5 - 10X_+^3 + 15X_+ + 8) + \rho_c & \text{for } r_c \le r \le r_+, \\ \rho_+ & \text{for } r \ge r_+, \end{cases} \qquad (2.8)$$

with

$$r_c \equiv \frac{r_+ + r_-}{2}, \qquad w \equiv \frac{r_+ - r_-}{2},$$
$$X_\pm \equiv \frac{r - r_c \mp w/2}{w/2}. \qquad (2.9)$$

Among the parameters above, $\rho_c \equiv \rho(r_c)$ cannot be fixed in advance. It is determined as an eigenvalue of Einstein equations (2.3) and (2.4) with the boundary condition $m(r_+) = 4\pi G\rho_+(a_+r_+)^3/3$ and $f(r_+) = 0$. We define the times t_1, t_2, t_3, and t_4 as follows: the photon passes $r = r_+$ from V_+ to V_s at $t = t_1$, passes $r = r_-$ from V_s to V_- at $t = t_2$, passes the other side of $r = r_-$ from V_- to V_s at $t = t_3$, and passes the other side of $r = r_+$ from V_s to V_+ at

$t = t_4$. Examples of initial and evolved configurations of $\rho(t, r)$ are shown in Fig. 1.

Our model parameters are the background density parameter, the density contrast, the physical radius in units of the Hubble radius, and the width of the shell in units of the comoving radius of the void/lump,

$$\Omega_4 \equiv \frac{8\pi G\rho_+(t_4)}{H_+^2(t_4)}, \qquad \delta_4 \equiv \frac{\rho_-(t_4)}{\rho_+(t_4)} - 1, \qquad (2.10)$$
$$R(t_4, r_c)H_+(t_4), \qquad w/r_c,$$

at the exit time t_4 of the photon. The initial parameters Ω_i, δ_i, and r_c are obtained by iterative integration of the field equation (2.3) with (2.10).
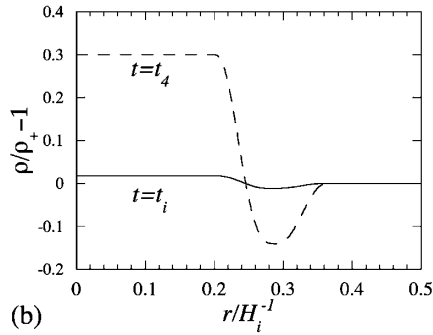

FIG. 1.   Examples of initial and evolved profiles of $\rho(t, r)$. (a) and (b) correspond to a void ($\delta < 0$) and a lump ($\delta > 0$), respectively.

C. Temperature anisotropy

The wave 4-vector k^μ of a photon satisfies the null geodesic equations,

$$k^\mu = \frac{dx^\mu}{d\lambda}, \qquad k^\mu k_\mu = 0, \qquad (2.11)$$

$$\frac{dk^\mu}{d\lambda} + \Gamma^\mu_{\nu\sigma} k^\nu k^\sigma = 0, \qquad (2.12)$$

where λ is an affine parameter. In what follows, we only consider a CMB photon which passes the void/lump center, $r = 0$. Then the geodesic equations (2.11) and (2.12) with the metric (2.2) yield

$$\frac{dt}{d\lambda} = k^t, \qquad \frac{dr}{d\lambda} = k^r, \qquad k^\theta = k^\varphi = 0, \qquad (2.13)$$

$$k^r = \epsilon \frac{\sqrt{1+f}}{R'} k^t, \qquad \epsilon \equiv \text{sign}\left(\frac{dr}{dt}\right), \qquad (2.14)$$

$$\frac{dk^t}{d\lambda} = -\frac{\dot{g}_{rr}}{2}(k^r)^2, \qquad \frac{d}{d\lambda}(g_{rr}k^r) = \frac{g'_{rr}}{2}(k^r)^2,$$

$$g_{rr} \equiv \frac{(R')^2}{1+f}. \qquad (2.15)$$

For the period $t_2 < t < t_3$ in V_-, the evolution of k^t_- and the crossing time are given by

$$k^t_- \propto \frac{1}{a_-}, \qquad \int_{t_2}^{t_3} \frac{dt}{a_-} = \frac{2}{C}(Cr_-). \qquad (2.16)$$

For the periods $t_1 < t < t_2$ and $t_3 < t < t_4$ in V_s we numerically solve the geodesic equations and the field equations simultaneously. First, we discretize the radial coordinate into N elements,

$$r_i = r_- + (i-1)\Delta r, \qquad i = 1, \ldots, N,$$

$$\Delta r = \frac{r_+ - r_-}{N-1}, \qquad (2.17)$$

and $R(t, r)$ into $R_i(t) \equiv R(t, r_i)$.

Next, we rewrite the geodesic equations (2.13), (2.14), and (2.15) and the field equations (2.3) and (2.5) as differential equations of r,

$$\frac{dt}{dr} = \frac{\epsilon R'}{\sqrt{1+f}}, \qquad (2.18)$$

$$\frac{dk^t}{dr} = -\frac{\epsilon \dot{R}'}{\sqrt{1+f}} k^t, \qquad (2.19)$$

$$\frac{d}{dr}(g_{rr}k^r) = \frac{g'_{rr}}{2} k^r, \qquad (2.20)$$

$$\frac{dR_i}{dr} = \dot{R}_i\left(\frac{dt}{dr}\right), \qquad (2.21)$$

$$\frac{dR'_i}{dr} = \dot{R}'_i\left(\frac{dt}{dr}\right), \qquad (2.22)$$

where $\dot{R}$, $\dot{R}'$, and $(\frac{dt}{dr})$ are given by (2.3), (2.5), and (2.18), respectively.

Finally, we carry out numerical integration of (2.18), (2.19), (2.21), and (2.22) using the fourth-order Runge-Kutta method to obtain the solutions of $t(r)$, $k^t(r)$, $R_i(t(r))$, and $R'_i(t(r))$. To estimate the numerical precision, we also numerically solve Eq. (2.20) and check how the solution satisfies (violates) the null condition (2.14).

The energy of a photon passing through the homogeneous background without a void/lump is

$$k^t_+ \propto \frac{1}{a_+}. \qquad (2.23)$$

Then the temperature fluctuation caused by a void/lump can be written as

$$\frac{\Delta T}{T} = \frac{k^t}{k^t_+} - 1. \qquad (2.24)$$

III. RESULTS

Figure 2 shows temperature fluctuations of photons passing through a void/lump for comoving observers at each $r = $ constant. The amplitude of fluctuations temporarily increases to $|\Delta T/T| \sim 10^{-3}$, but it finally reduces to $\sim 10^{-5}$ at the edge of the shell because the mass of the void/lump is compensated.

In what follows, we discuss only the values of $\Delta T/T$ measured by a comoving observer outside a void/lump. For a void, as Fig. 3(a) indicates, the temperature fluctuation $\Delta T/T$ is always negative regardless of the values of Ω_4. For a fixed radius, $|\Delta T/T|$ decreases as the width w/r_c of the void shell increases. We find that our results are consistent with those for a thin-shell homogeneous void in the quasilinear regime [10]. To see nonlinear effects, in Figs. 3 (b) and 3(c) we plot $\Delta T/T$ obtained from a linear perturbation analysis, a second-order perturbation analysis, and our fully nonlinear analysis. We find that higher-order effects are important and they enhance $|\Delta T/T|$ for a void, particularly for large Ω_4.

For a lump, as Fig. 4(a) indicates, the temperature fluctuation $\Delta T/T$ is positive for low background density, but it can be negative for high background density. In other words, lumps at low-z blueshift the CMB photons, whereas lumps at high-z redshift them. This behavior of $\Delta T/T$ in the quasilinear regime can be interpreted as follows. First, let us consider a perturbative case $|\delta_4| \ll 1$ for which the linear integrated Sachs-Wolfe (ISW) effect [12] dominates $\Delta T/T$. Then one can show that $\Delta T/T$ vanishes for $\Omega_4 = 0$ (de Sitter) because no matter fluctuation exists, and for
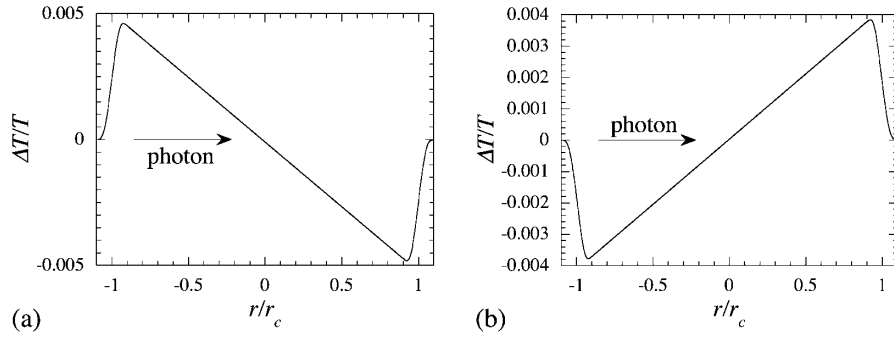
FIG. 2.   Temperature fluctuations of photons passing through the center of a large void (a) and a large lump (b) for comoving observers at each $r =$ constant. The parameters are $\delta_4 = \mp 0.3$, $\Omega_4 = 0.24$, $R_4(r_c) = 0.1H_4^{-1}$, and $w/r_c = 0.1$. The subscript 4 denotes quantities at the time t_4 when a CMB photon exits the edge of a void/lump. The arrow indicates the traveling direction of a CMB photon.

$\Omega_4 = 1$ (Einstein–de Sitter) because the Newtonian gravitational potential freezes in the Einstein–de Sitter universe. Therefore, $\Delta T/T$ cannot be a monotonic function of Ω_4 for $0 < \Omega_4 < 1$. In fact, as one can see in Fig. 4(a), the ISW contribution has a peak as a function of Ω_4 for a fixed δ_4. Next, let us consider a quasilinear case $0.1 \lesssim |\delta_4| \lesssim 1$. For small Ω_4, the nonlinear RS effect is not important because matter fluctuations are small. However, for large Ω_4, the nonlinear RS effect dominates the linear ISW effect, which vanishes for $\Omega_4 = 1$. Our numerical analysis shows that the nonlinear RS effect reduces the temperature of the CMB photons, which reconfirms the previous semianalytic

result for lumps in the Einstein–de Sitter universe [3]. Thus, one can interpret that negative $\Delta T/T$ in the $\Omega_4 = 1$ background for a void/lump [in Figs. 3(a)/4(a)] is caused by the nonlinear RS effect alone. It should also be noted that our result is consistent with the previous one obtained from a second-order perturbation analysis for a void/lump in accelerating universes [11].

Figures 4(b) and 4(c) shows nonlinear effects for a lump: higher-order effects are still important, but they reduce the amplitude of $\Delta T/T$ in contrast to the case for a void in Figs. 3(b) and 3(c).
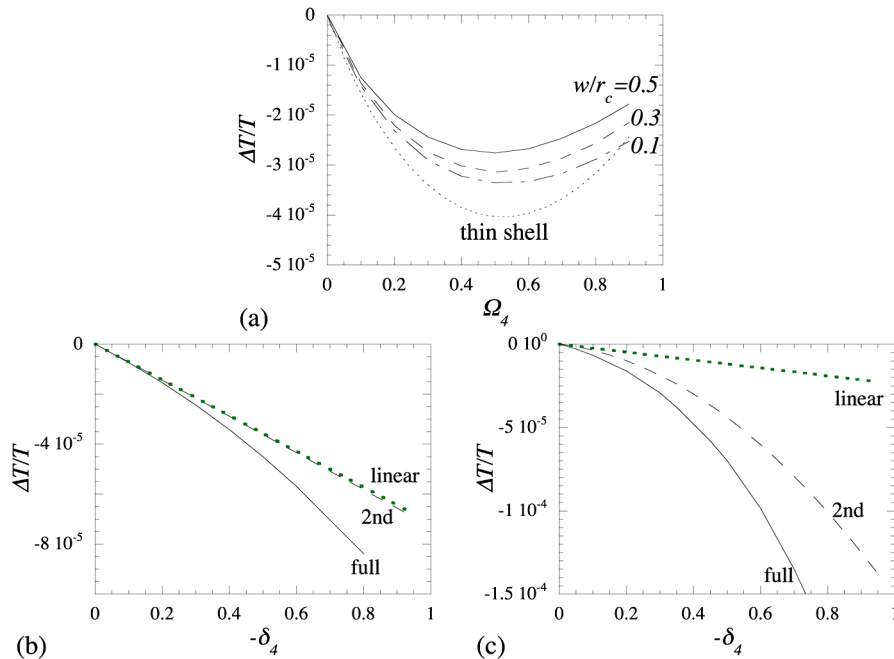

FIG. 3 (color online).   Temperature fluctuations of CMB photons passing through the center of a large void with $R_4(r_c) = 0.1H_4^{-1}$ for a comoving observer outside the void. (a) $\Delta T/T$ as a function of Ω_4 for $\delta_4 = -0.3$. The dotted line indicated by "thin shell" shows $\Delta T/T$ for the thin-shell model [10]. (b) and (c) $\Delta T/T$ as a function of $-\delta_4$ for $\Omega_4 = 0.24$ and for $\Omega_4 = 0.9$, respectively; we put $w/r_c = 0.3$ for both cases. The dotted lines and the dashed lines represent the values obtained from a linear perturbation analysis, and a second-order perturbation analysis [11], respectively.
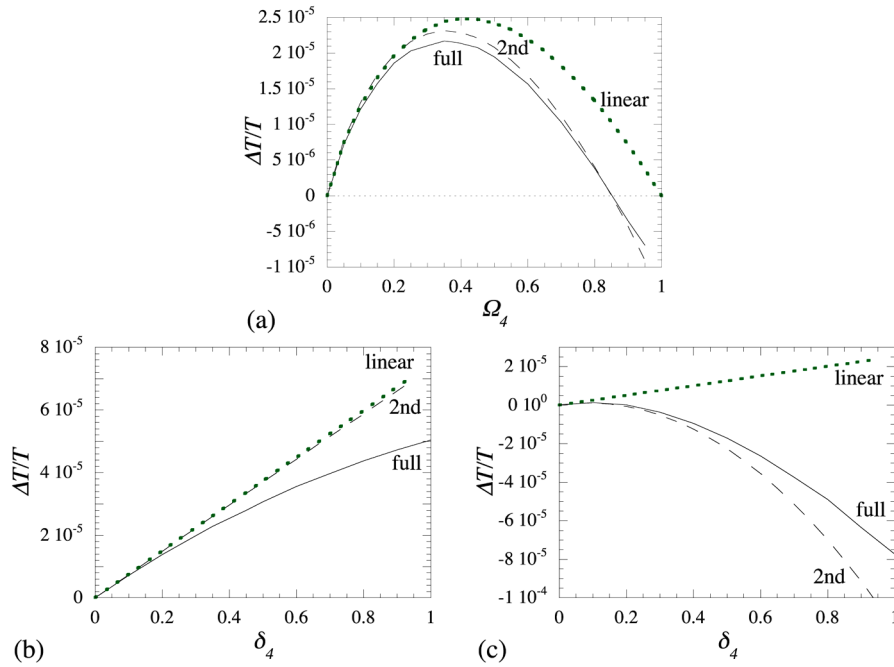
FIG. 4 (color online). Temperature fluctuations of CMB photons passing through the center of a large lump with $R_4(r_c) = 0.1H_4^{-1}$ and $w/r_c = 0.15$ for a comoving observer outside the lump. The dotted lines and the dashed lines represent the values obtained from a linear perturbation analysis, and a second-order perturbation analysis [11], respectively. (a) $\Delta T/T$ vs Ω_4 for $\delta_4 = 0.3$. (b) and (c) $\Delta T/T$ vs δ_4 for $\Omega_4 = 0.24$ and for $\Omega_4 = 0.9$, respectively.

IV. CONCLUDING REMARKS

We have studied the CMB anisotropy caused by spherically symmetric nonlinear structures in flat universes with dust and cosmological constants. Specifically, by modeling a time-evolving spherical compensated void/lump by Lemaitre-Tolman-Bondi spacetimes, we have solved the null geodesic equations with the Einstein equations numerically.

We have found that a nonlinear void redshifts the CMB photons that pass through it regardless of its location. In contrast, a compensated nonlinear lump blueshifts (or redshifts) the CMB photons if it is located near (or sufficiently far from) us.

Our result for the temperature anisotropy due to a void is roughly consistent with the previous one based on a thin-shell approximation. We have also shown that $|\Delta T/T|$ decreases as the shell thickness increases for fixed δ.

We have checked that our results are also consistent with the ones based on a linear/second-order perturbation method for small $|\delta|$. It turned out that nonlinear (higher-order) effects are important even in the quasilinear regime $|\delta| \gtrsim 0.3$.

Our results indicate that, if a quasilinear ($|\delta| \sim 0.3$) and large size ($R \sim 0.1H^{-1}$) void/lump could exist, they would be observed as a cold or hot spot at the level of $\Delta T/T \sim 10^{-5}$ in the CMB sky. In such a case fully nonlinear and relativistic analysis is necessary.

[1] M. J. Rees and D. W. Sciama, Nature (London) **217,** 511 (1968).

[2] H. Sato, Prog. Theor. Phys. **73,** 649 (1985); K. L. Thompson and E. T. Vishniac, Astrophys. J. **313,** 517 (1987); E. Martínez-Gonzáles, J. L. Sanz, and J. Silk, *ibid.* **355,** L5 (1990).

[3] E. Martínez-Gonzáles and J. L. Sanz, Mon. Not. R. Astron.

Soc. **247,** 473 (1990); E. Martínez-Gonzáles, J. L. Sanz, and J. Silk, Astrophys. J. **436,** 1 (1994).

[4] M. Panek, Astrophys. J. **388,** 225 (1992); J. V. Arnau, M. J. Fullana, L. Monreal, and D. Sáez, *ibid.* **402,** 359 (1993); A. Mészáros, *ibid.* **423,** 19 (1994); R. Tuluie and P. Laguna, *ibid.* **445,** L73 (1995); R. Tuluie, P. Laguna, and P. Anninos, *ibid.* **463,** 15 (1996); A. Mészáros and

Z. Molinár, *ibid.* **470**, 49 (1996); M. J. Fullana, J. V. Arnau, and D. Sáez, Mon. Not. R. Astron. Soc. **280**, 1181 (1996); X. Shi, L. M. Widrow, and L. J. Dursi, *ibid.* **281**, 565 (1996); C. Baccigalupi, L. Amendola, and F. Occhionero, *ibid.* **288**, 387 (1997); S. L. Vadas, *ibid.* **299**, 285 (1998); N. Sakai, N. Sugiyama, and J. Yokoyama, Astrophys. J. **510**, 1 (1999); A. Cooray, *ibid.* **574**, 19 (2002); Phys. Rev. D **65**, 083518 (2002); **65**, 103510 (2002).

 [5] M. Tegmark, A. de Oliveira-Costa, and A. J. S. Hamilton, Phys. Rev. D **68**, 123523 (2003); A. de Oliveira-Costa, M. Tegmark, M. Zaldarriaga, and A. Hamilton, *ibid.* **69**, 063516 (2004).

 [6] P. Vielva, E. Martínez-González, R. B. Barreiro, J. L. Sanz, and L. Cayon, Astrophys. J. **609**, 22 (2004); M. Cruz, E. Martínez-González, P. Vielva, and L. Cayon, Mon. Not. R. Astron. Soc. **356**, 29 (2005).

 [7] H. K. Eriksen, F. K. Hansen, A. J. Banday, K. M. Gόrski, and P. B. Lilje, Astrophys. J. **605**, 14 (2004); F. K. Hansen, A. Balbi, A. J. Banday, K. M. Gόrski, Mon. Not. R. Astron. Soc. **354**, 905 (2004).

 [8] A. Cooray and N. Seto, J. Cosmol. Astropart. Phys. 12 (2005) 004; K. Tomita, Phys. Rev. D **71**, 083504 (2005); **72**, 043526 (2005); **72**, 103506 (2005); K. T. Inoue and J. Silk, Astrophys. J. **648**, 23 (2006).

 [9] L. Rudnick, S. Brown, and L. R. Williams, Astrophys. J. **671**, 40 (2007).

 [10] K. T. Inoue and J. Silk, Astrophys. J. **664**, 650 (2007).

 [11] K. Tomita and K. T. Inoue, Phys. Rev. D **77**, 103522 (2008).

 [12] R. K. Sachs and A. M. Wolfe, Astrophys. J. **147**, 73 (1967).